Exploring Dynamical Status and High Energy Phenomena of Merging Galaxy Clusters with Multi-band Observations and Numerical Simulations

Motokazu Takizawa

(Yamagata University)

Abell 2319: Sugawara,Takizawa, & Nakazawa (2009)

ZwCl0823.2+0425 Field: Watanabe, Takizawa et al. (2011)

Mass Estimation: Takizawa, Nagino, & Matsushita (2010)

High Energy Phenomena of Clusters of Galaxies

Non-thermal radio emission from merging clusters of galaxies

synchrotron radio

$\gamma \sim 10^4$ electrons + 0.1-10μG B

Hard X-ray will be emitted through Inverse compton with CMB

Coma Cluster

Deiss et al.1996

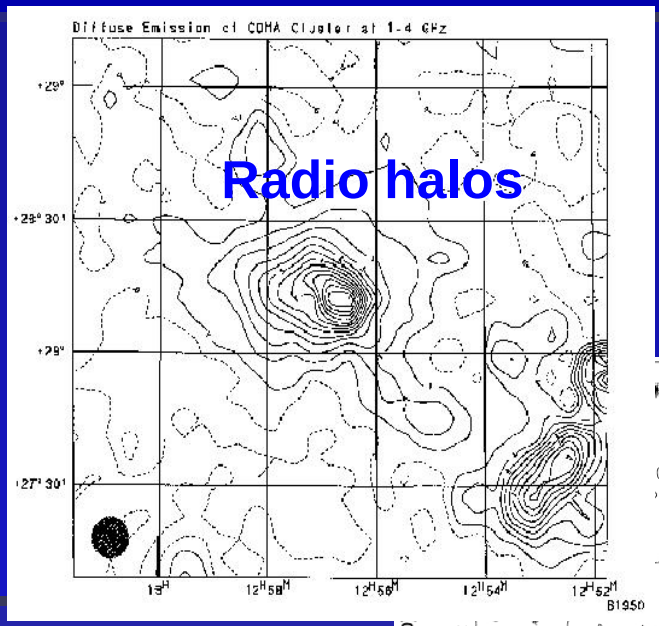

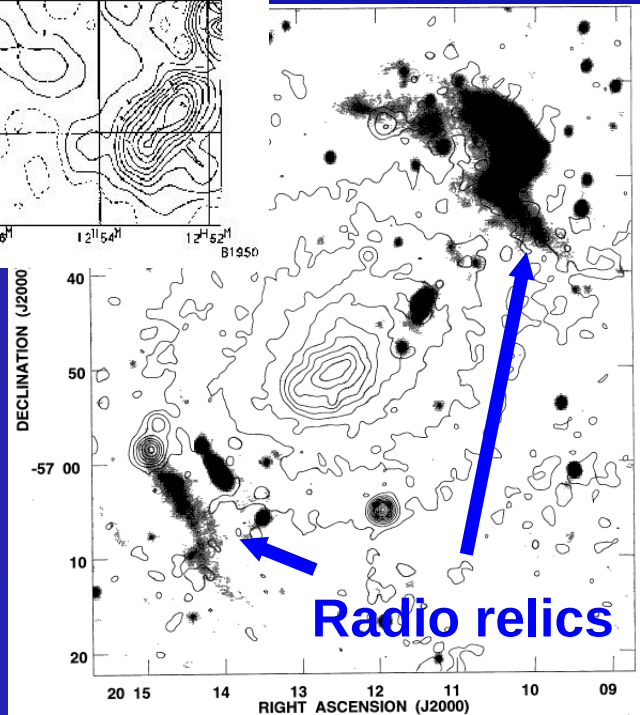

A3667
Röttgeringet al.1997

Hard X-ray observations

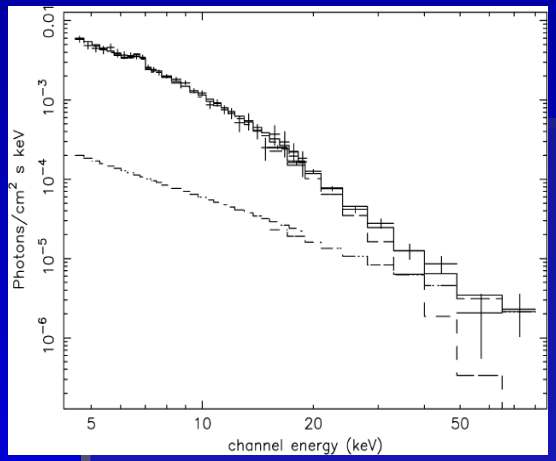

Detection of Non-thermal hard X-ray from Coma ??
(Fusco-Femiano et al. 1999, 2005etc)

Beppo-SAX（1996-2002）

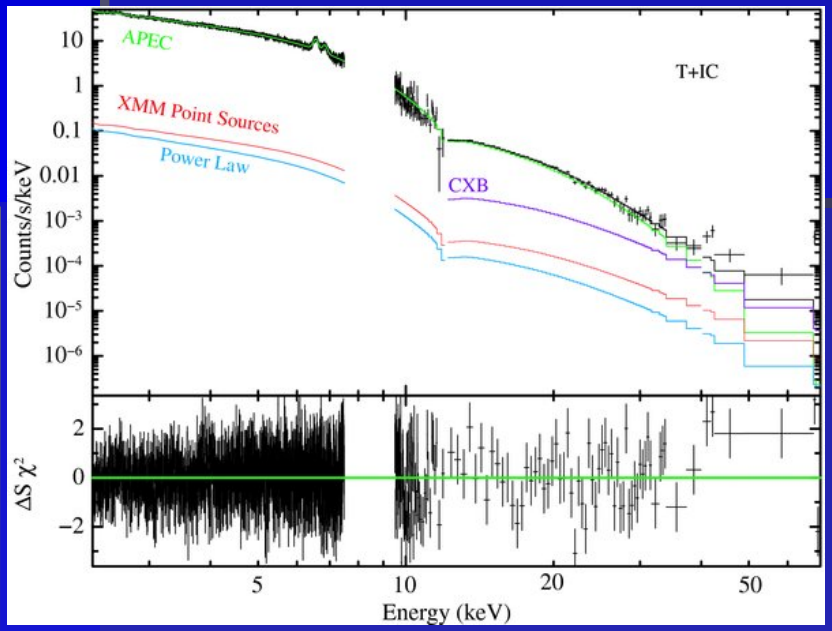

No significant non-thermal component.
Tighter upper limit than the detection by B-SAX
(Wik et al. 2009)

Suzaku（2005～）

Abell 2319

- Nearby (z=0.0557) well-known merging cluster with a giant radio halo
- Two subgroups are found in radial velocity distribution of the member galaxies

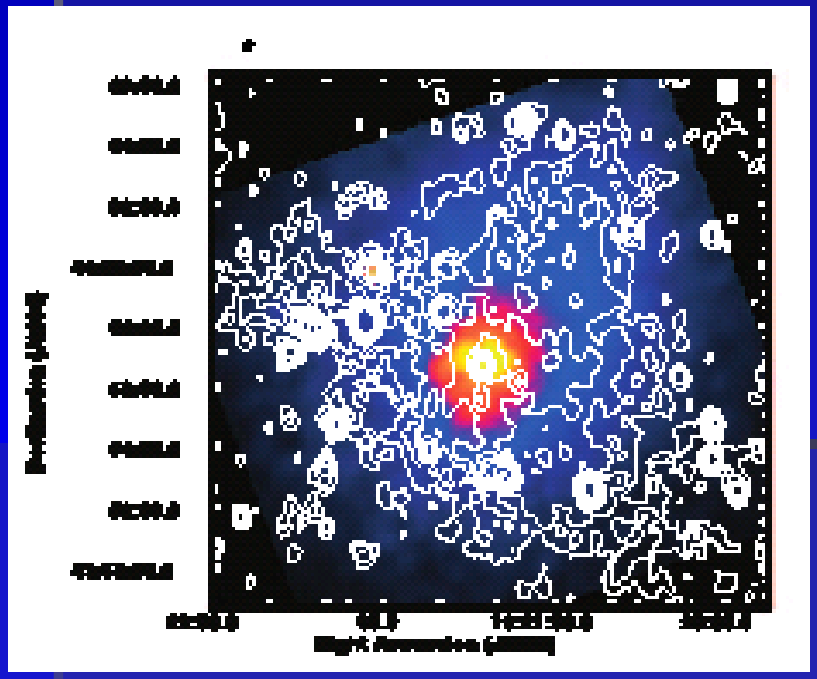

Rosat X-ray image (colors)
Radio image (contours)
Feretti et al. 1997

Lline-of-sight velocity distribution of member galaxies

A2319A
15727±139km/s

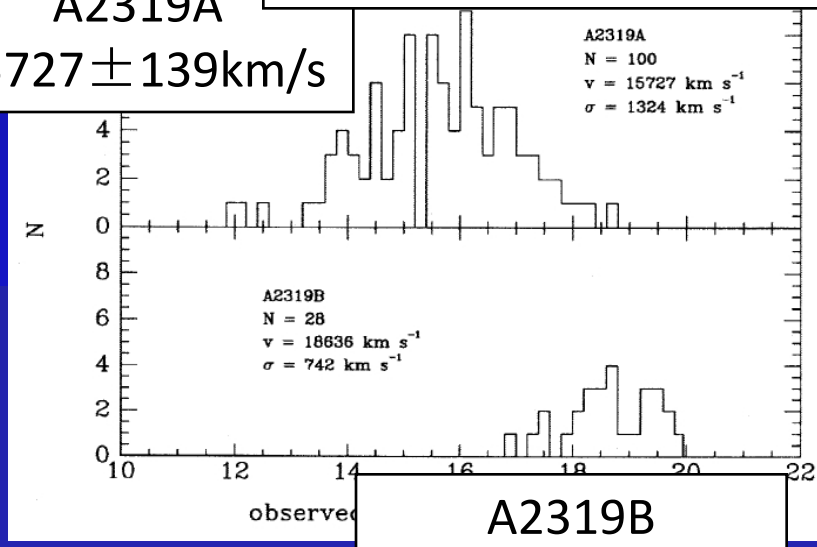

A2319B
18636±151km/s

Oegerle et al.1995

Line-of-sight Velocities of the ICM

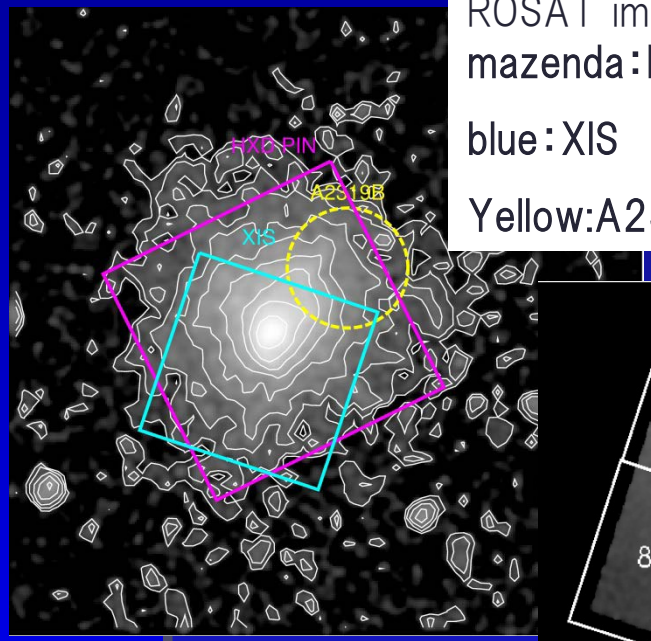

ROSAT image
mazenda：HXD PIN、
blue：XIS
Yellow:A2319B

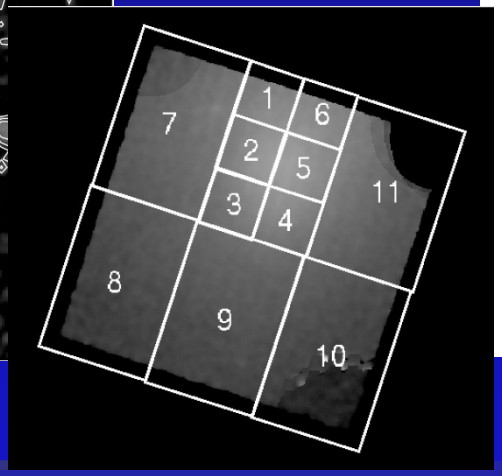

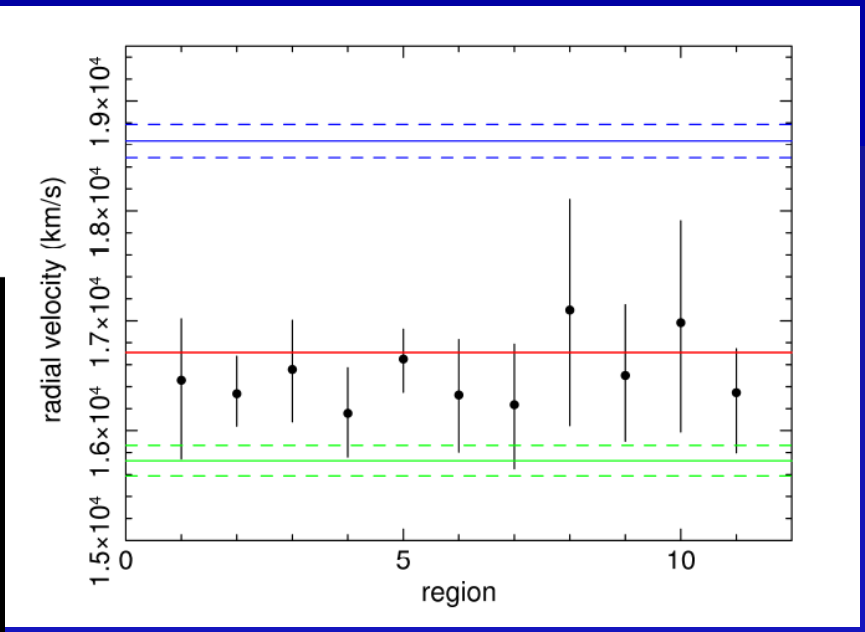

- It is clear that the observed velocities are different from that of A2319B subgroup.
- No significant velocity difference is detected within the observed region.
- $\Delta v < 940^{+1083}_{-1131}$ km/s. (cf. $c_s \sim 1700$ km/s)

Line-of-sight velocity

Blue: A2319B subgroup
Green: A2319A subgroup
Red: A2319

Wide band spectrum

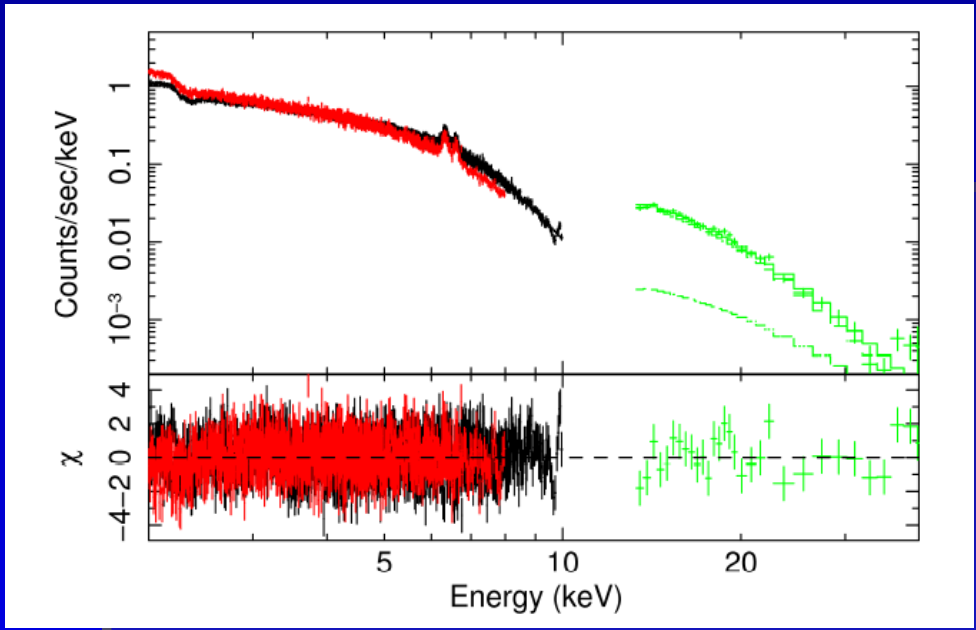

Wide band spectrum fitted with APEC+Powerlaw model

Black: XIS FI
Red: XIS BI
Green: PIN

Flux of a power-law component in 10-40 keV and its upper limits

model	flux (erg s^{-1} cm^{-2})	upper limit (erg s^{-1} cm^{-2})
$1kT + PL(1.92)$	$1.1^{+0.8+1.3}_{-0.8-1.1} \times 10^{-11}$	$< 2.6 \times 10^{-11}$
$1kT + PL(2.4)$	$1.5^{+1.2+1.9}_{-1.2-2.1} \times 10^{-11}$	$< 3.8 \times 10^{-11}$
$2kT + PL(1.92)$	$0.0^{+3.7+2.2}_{-0.0-0.0} \times 10^{-11}$	$< 4.3 \times 10^{-11}$
$2kT + PL(2.4)$	$0.0^{+2.2+3.9}_{-0.0-0.0} \times 10^{-11}$	$< 4.5 \times 10^{-11}$

The lower limit of the magnetic field strength

model	$B(\mu G)$
$1kT + PL(1.92)$	> 0.19
$1kT + PL(2.4)$	> 0.27
$2kT + PL(1.92)$	> 0.14
$2kT + PL(2.4)$	> 0.25

Energy Budget of the Intracluster space

Thermal Energy

- ROSAT image → $n_e(r)$
- kT=10keV

$$U_{\rm th} = 0.4 \times 10^2 \ {\rm eV/cm^3}$$

Abell 2319

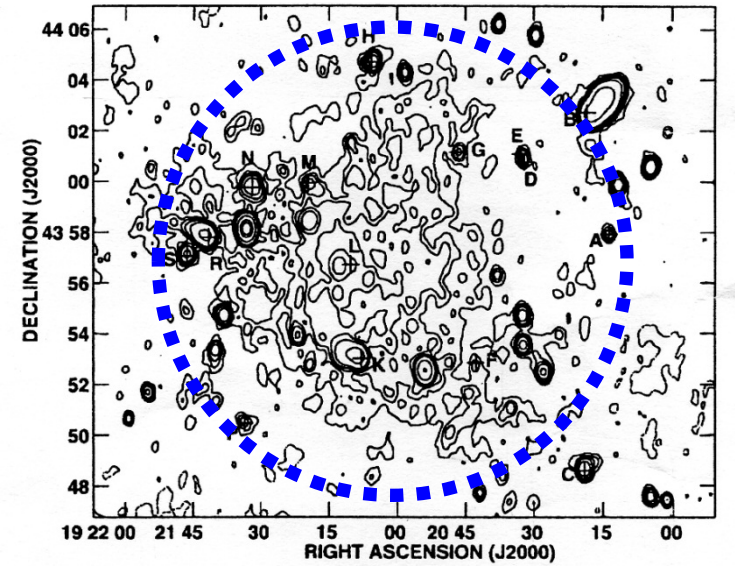

Feretti et al.1997

Magnetic Energy

- **Suzaku Results (>0.2μG)**

$$U_B > 0.1 \times 10^{-2} \ {\rm eV/cm^3}$$

$$\frac{U_{\rm th}}{U_B} < 2.0 \times 10^3$$

CR electrons ($5.7 \times 10^3 < \gamma < 1.1 \times 10^4$)

- Suzaku results (upper limit of hard X-ray)

$$U_e < 0.2 \times 10^{-1} \ {\rm eV/cm^3}$$

$$\frac{U_{\rm th}}{U_e} > 4.0 \times 10^4$$

ZwCl 0823.2+0425 Field

Optical image and the mass contours
With XIS FOV.

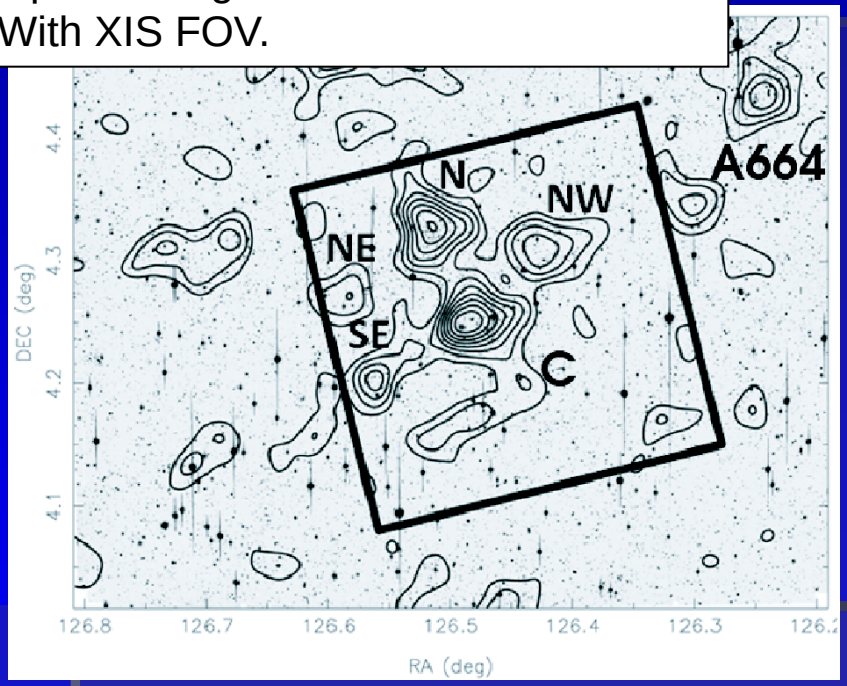

ROSAT image

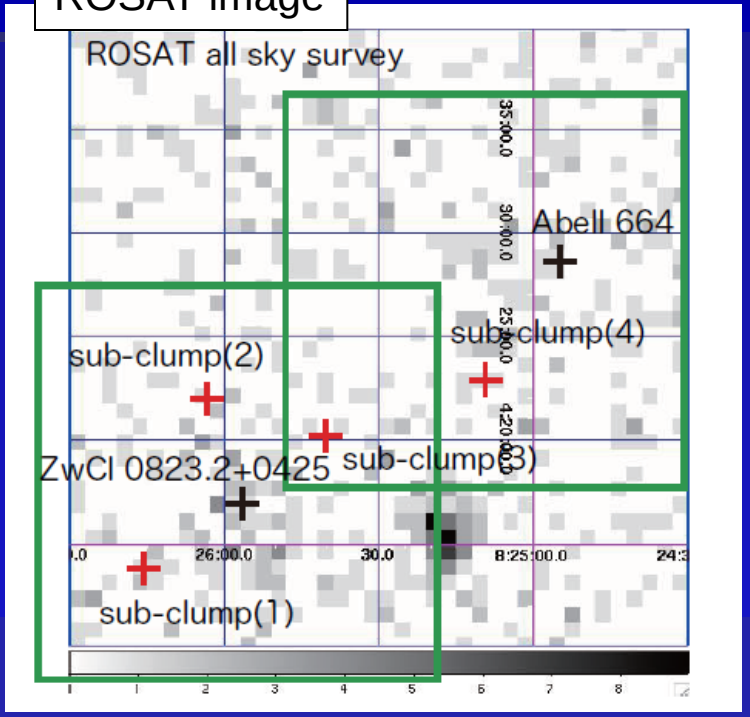

- Several dark halos were found by a weak lensing survey (Okabe et al. 2010).
- No deep X-ray image.
- L_X???, kT???, Metal Abundance????

Results(1)

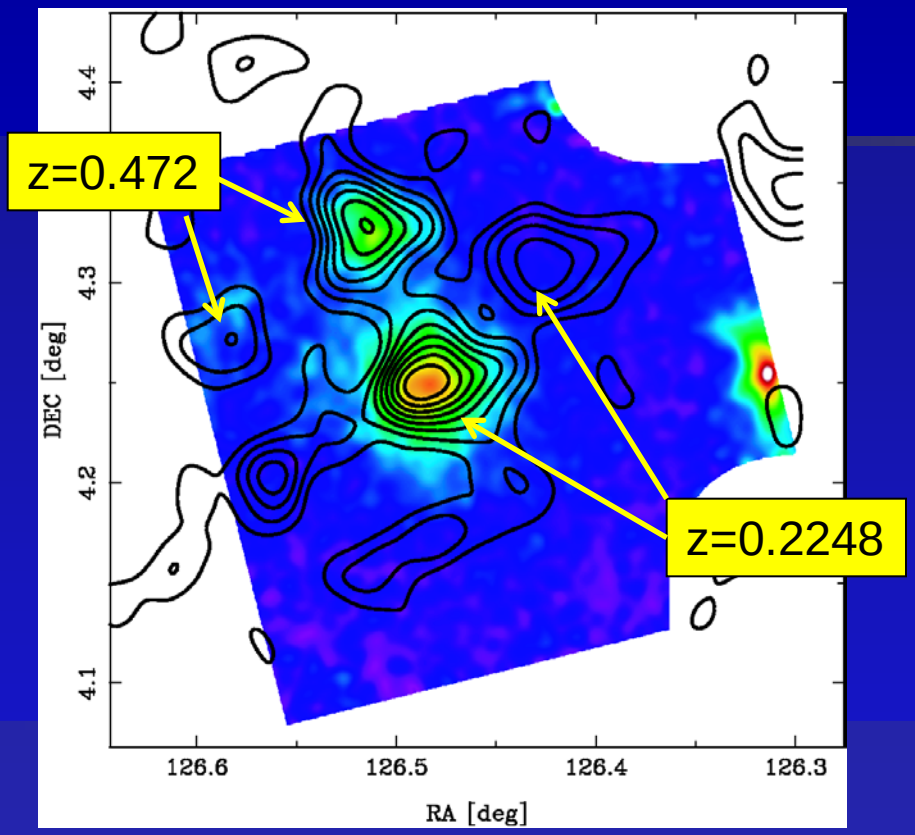

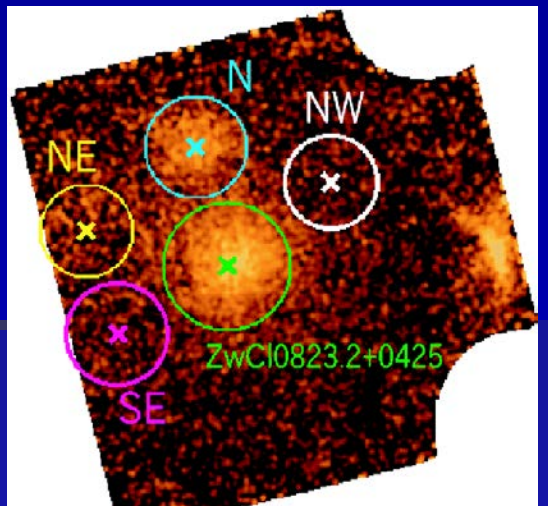

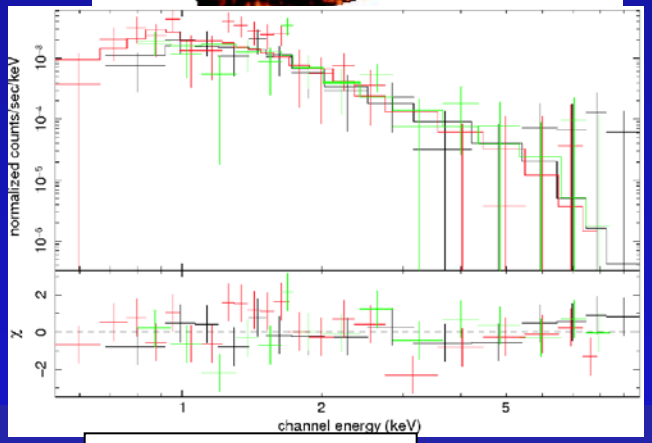

NW spectrum

- Significant excess X-ray signals except for SE
- kT determination except for SE
- Metal Abundance determination for C and N

Results(2)

M-T relation

Best fit (solid line)

$$M_{500}E(z) = 2.63^{+0.81}_{-0.63}\left(\frac{k_{\rm B}T}{5\ {\rm keV}}\right)^{2.38^{+0.78}_{-0.95}} \times 10^{14}h^{-1}M_{\odot}, \quad (8)$$

Assuming $M \propto T^{3/2}$ (solid line)

$$M_{500}E(z) = 2.47^{+0.69}_{-0.57}\left(\frac{k_{\rm B}T}{5\ {\rm keV}}\right)^{3/2} \times 10^{14}h^{-1}M_{\odot}, \quad (9)$$

Normalization is consistent with results of X-ray selected sample (Okabe et al. 2010)

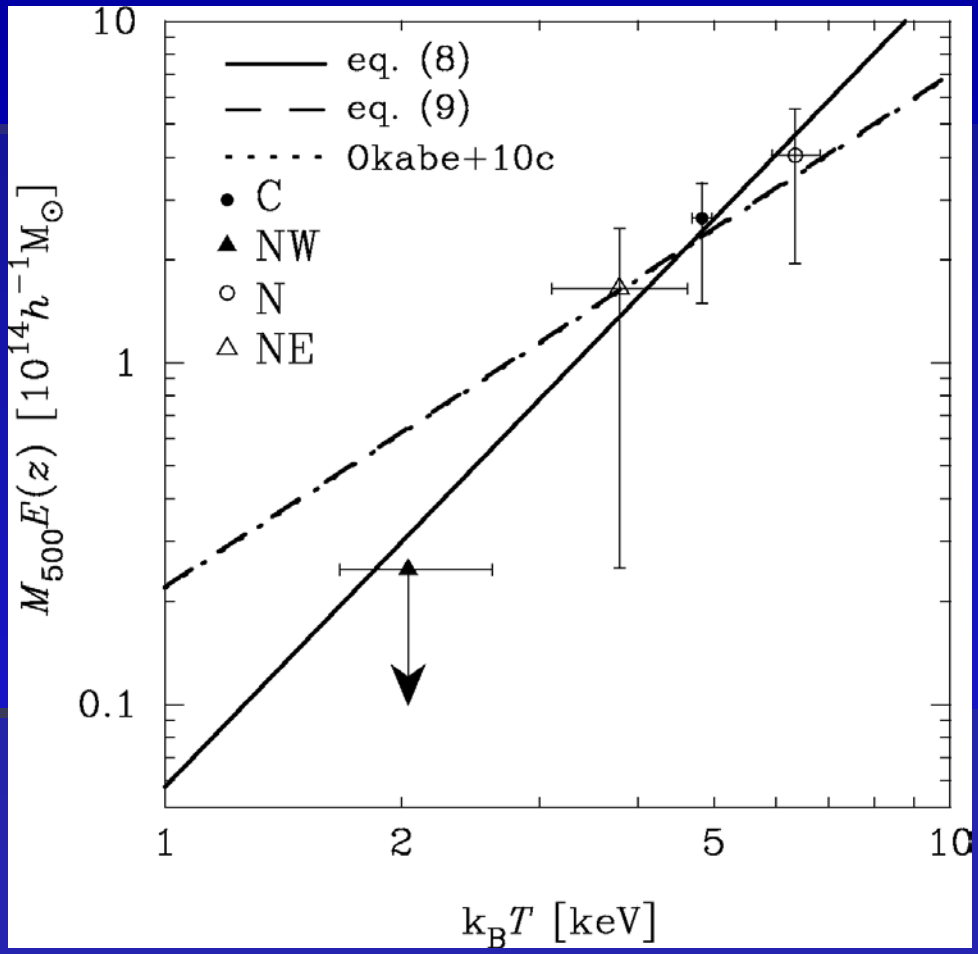

Mass Estimation of Merging Galaxy Clusters

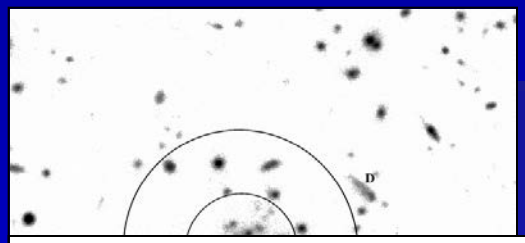

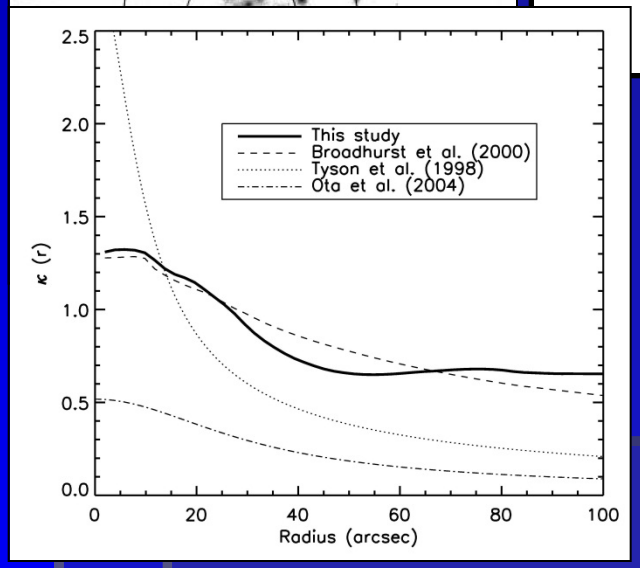

•CL 0024+17 (Ota et al. 2004, Broadhurst et al. 2000, Jee et al. 2007, Umetsu et al. 2010,,,,)
Sugnificant mass discrepancy within 200 kpc.
$M_{Lens}/M_X \sim 2\text{--}3$

•"Disturbed Clusters" tend to show larger mass discrepancy
（Zhang et al. 2010）.

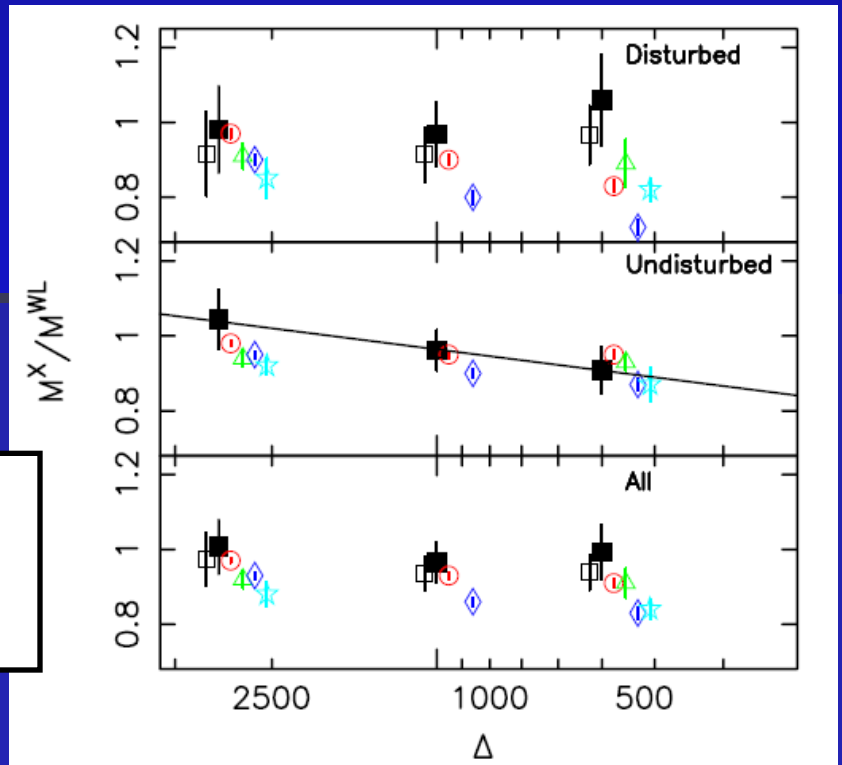

Simulation Data (N-body+ hydrodynamics)

Mass distribution

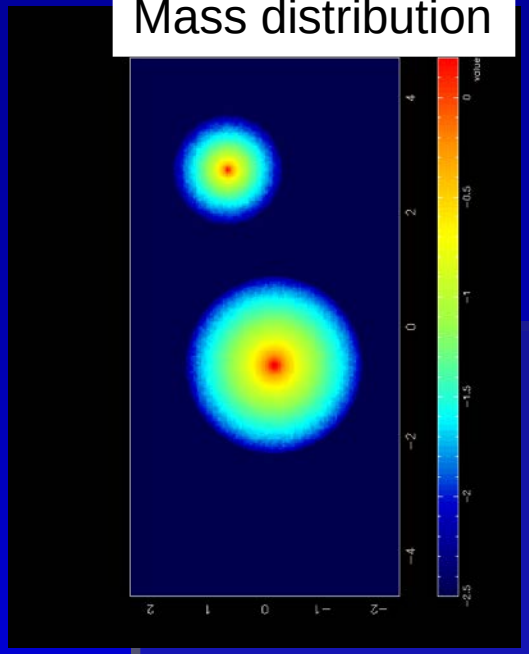

Gas density

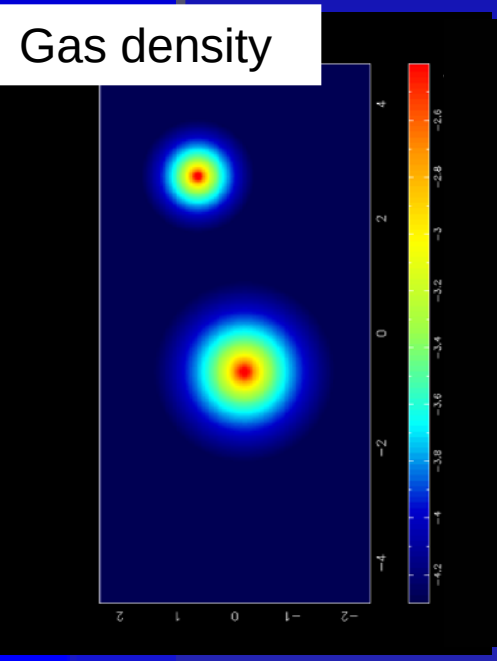

Gas temperature

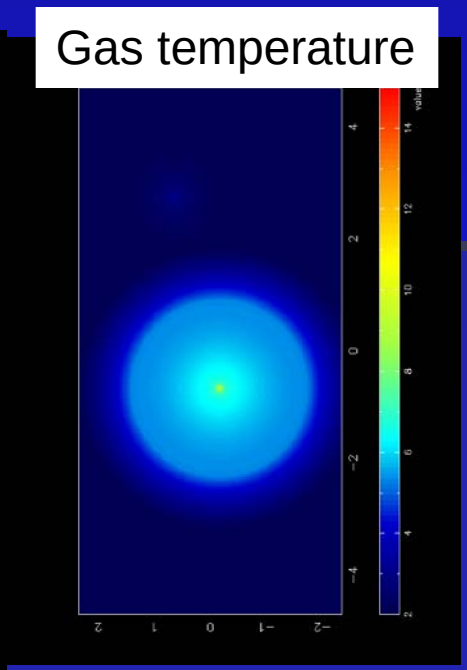

- N-body：Particle Mesh (PM) method
- self-gravity：FFT with isolated boundary conditions
- hydrodynamics：Roe TVD method
- number of grid points $256 \times 128 \times 128$
- Number of particles $256 \times 128 \times 128$ ($\fallingdotseq 4.2 \times 10^6$)

Mass estimation during core passage

X-ray data seen along the collision axis

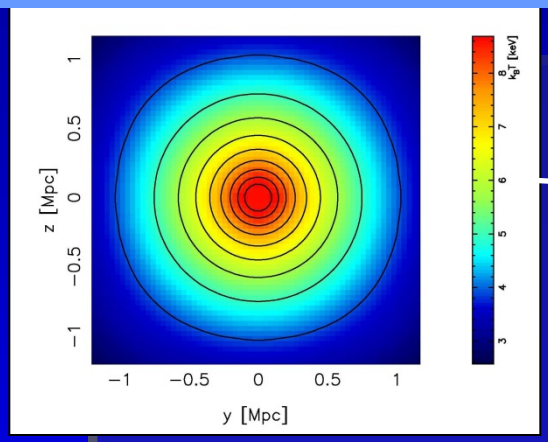

X-ray data seen from the direction perpendicular to the collision axis

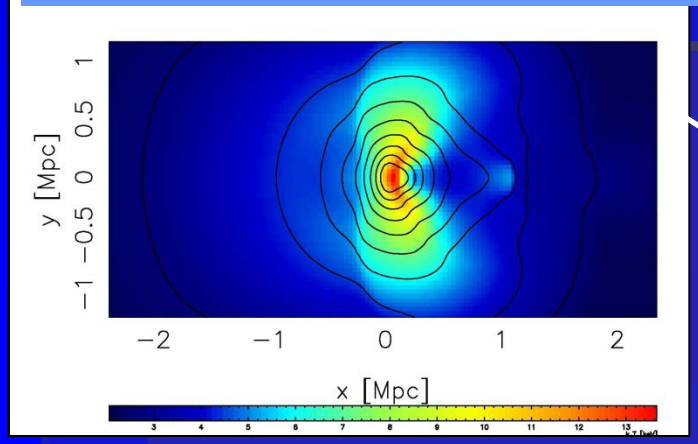

solid lines : M_{real}
dashed lines : M_X
asterisks : M_{virial}

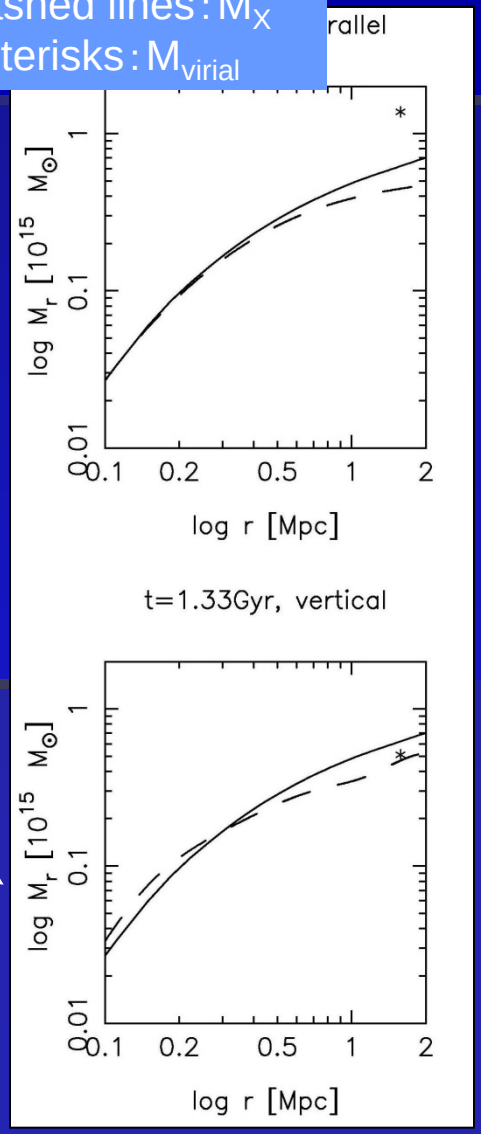

solid lines : M_X /M_{real}
asterisks : M_{virial} /M_{real}

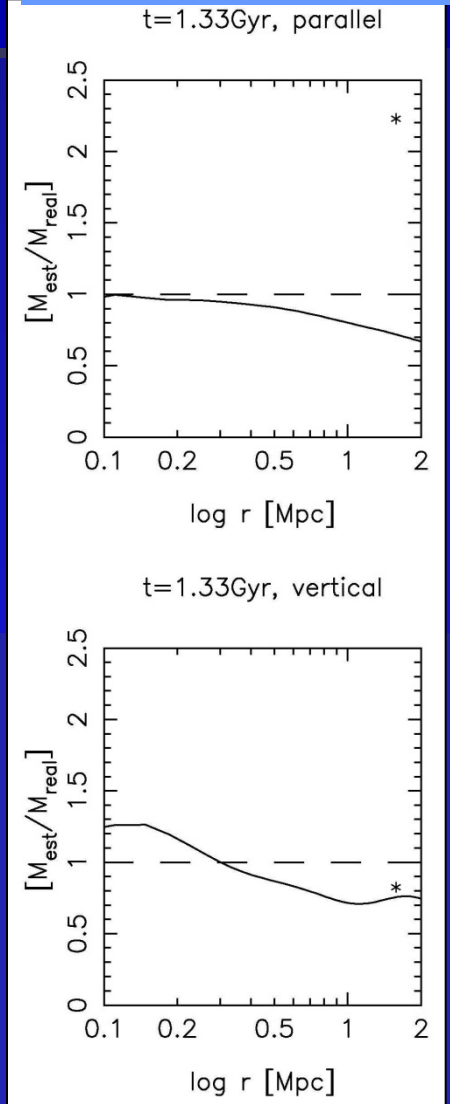

Mass estimation after core passage

X-ray data seen along the collision axis

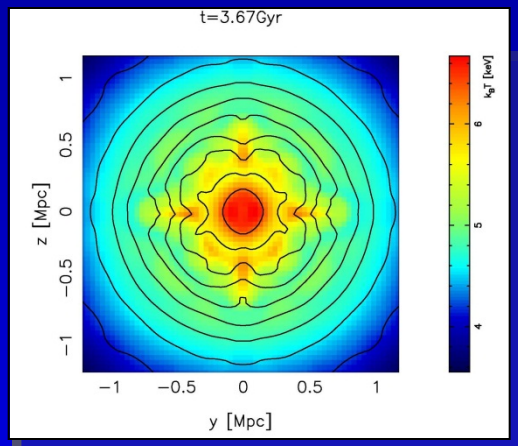

X-ray data seen from the direction perpendicular to the collision axis

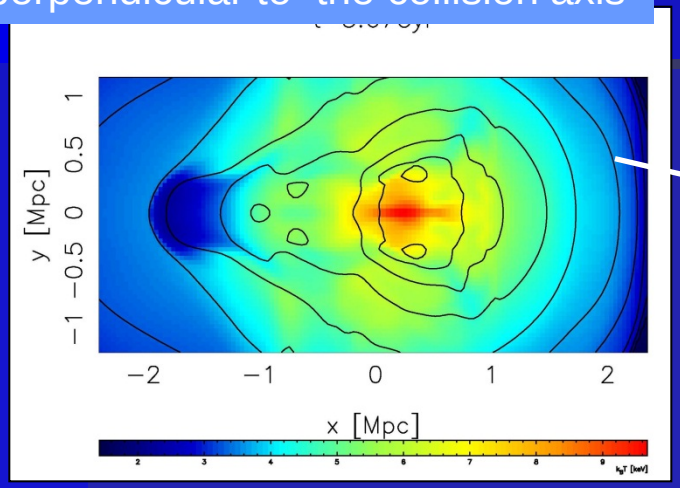

solid lines : M_{real}
Dashed lines : M_X
asterisks : M_{virial}

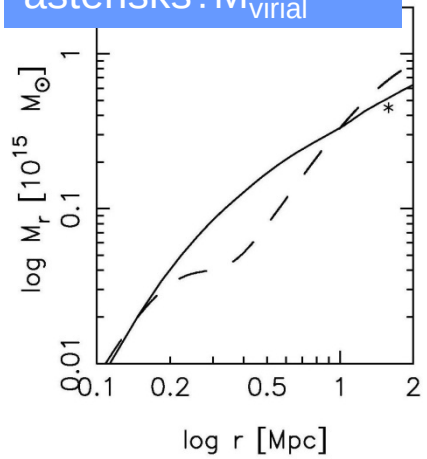

t=3.67Gyr, vertical

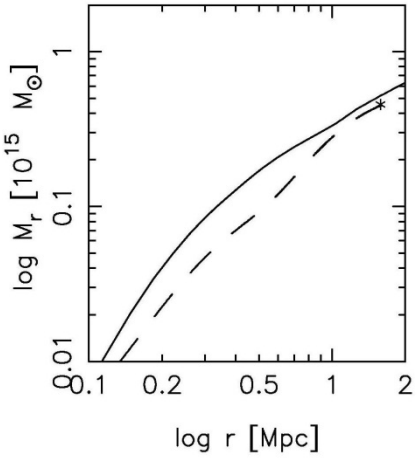

solid lines : M_X /M_{real}
asterisks : M_{virial} /M_{real}

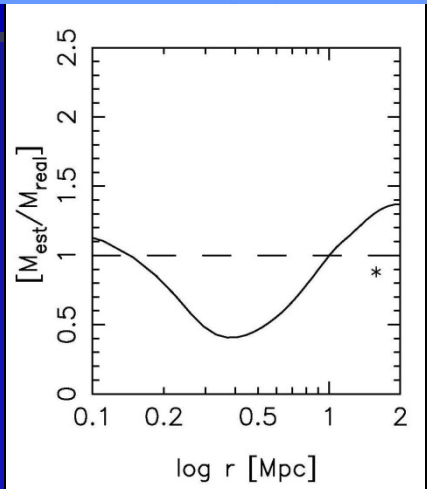

t=3.67Gyr, vertical

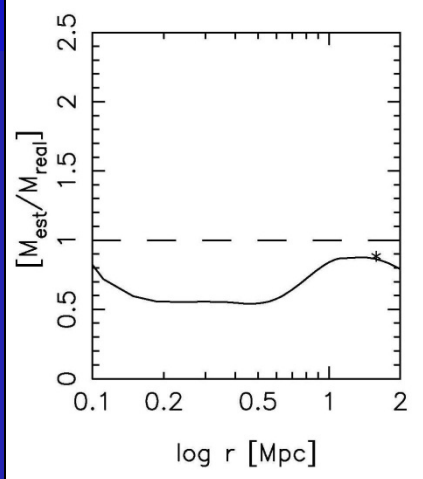

X-ray morphology and mass estimation uncertainity

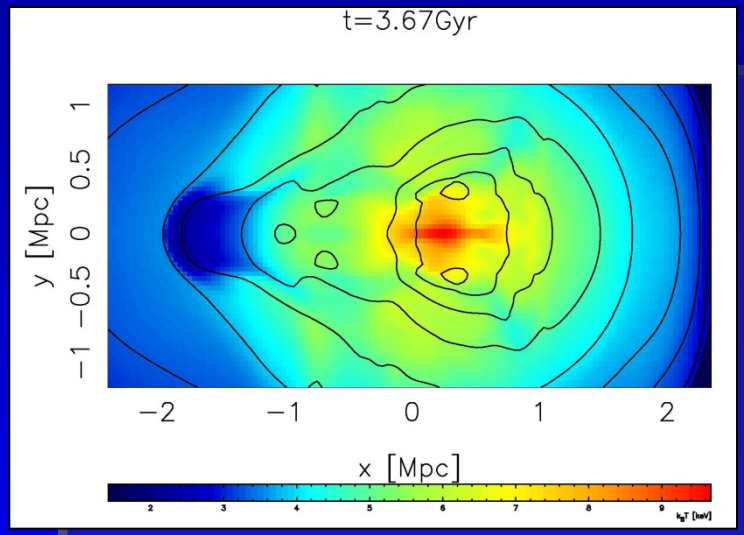

Solid lines: axial ratio of X-ray image within r

Dashed lines: M_X / M_{real}

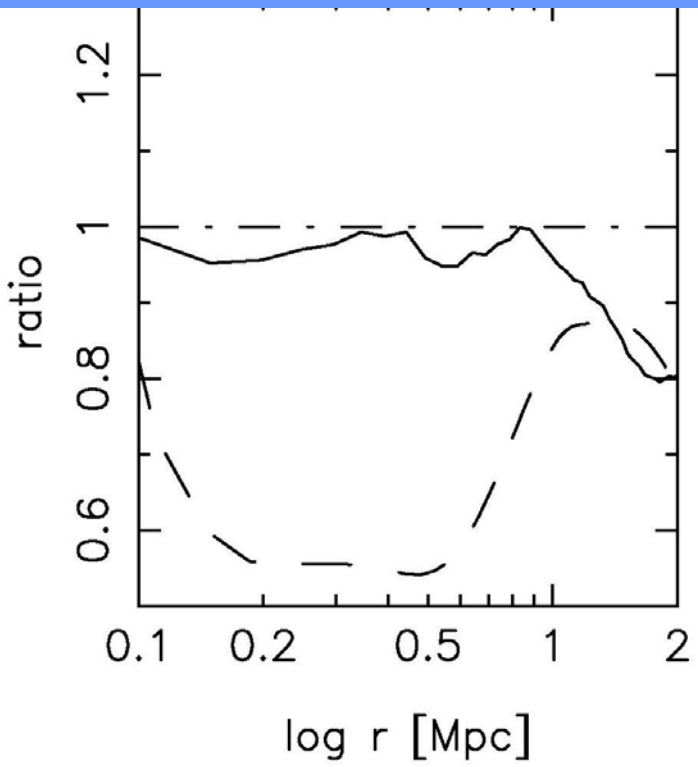

- Morpholgy depends on the radius within which it is estimated.
- This cluster looks “round” only in the inner part, but its mass is underestimated by over 40 %.

If this cluster is located at high redshift and hence only the inner part can be observed, what happens?

Summary

- A2319
  - Line-of-sight velocities of the ICM
  - Constraint of the energy density of the magnetic field and CR electrons through the non-thermal hard X-ray upper limit
- ZwCl0823.2+0425 Field
  - X-ray follow-up observation of weak-lensing-detected halos
  - Self-similar M-T relation consistent with X-ray selected sample
- Mass Estimation
  - Investigation of the Impact of the mergers on the mass estimation using N-body + hydrodynamical simulation data